Response of the Earth's Ionosphere to Solar Activity during Minimum, Moderate and Maximum Conditions

P. Thirupathaiah*., Lisy M. Thomas., Anil K. Das

Department of Physics, St. John's College, Agra, Uttar Pradesh, India

***Corresponding author**

DOI: https://doi.org/10.51584/IJRIAS.2025.10120047

Received: 28 December 2025; Accepted: 02 January 2026; Published: 15 January 2026

ABSTRACT

The response of Earth's ionosphere to the solar radiation during minimum, moderate and maximum solar activity conditions is studied using the International Reference Ionosphere (IRI-2016) model during the solar cycle 24. The altitude profiles of ion densities (O_2^+, NO^+, N^+, O^+), electron density (N_e), electron temperature (T_e) and ion temperature (T_i) are obtained from the IRI-2016 model on 4 January 2020 (F10.7 = 69.8, minimum), 4 January 2012 (F10.7 = 131.6, moderate) and 4 January 2014 (F10.7 = 253.3, maximum) at 45° latitude and 180° longitude in both the hemispheres for 12 noon local time from 60 km to 500 km altitude. It is found that the ion densities and electron density show a significant variation above 200km during minimum, moderate and maximum solar activity conditions, whereas below 200km the variation is more or less same. The electron temperature shows a significant variation above 300km, whereas below 300km the variation is more or less same. The ion temperature shows a significant variation between 150km and 450km, whereas below 150km and above 450km the variation is more or less same. It is also found that the values of densities of O_2^+, N^+, O^+ and electron are higher at 45°N than 45°S at 100-200km, 300-400km, above 150km, and above 150km, respectively, at other altitudes these values are higher at 45°S than 45°N. The values of NO^+ density, T_e and T_i are higher at 45°S than 45°N at almost all altitudes.

Keywords: Solar radiation, Earth's ionosphere, IRI-2016 empirical model

INTRODUCTION

The Earth's ionosphere is a region of the upper atmosphere (above 60 km), where free electrons and ions exist sufficiently in number to influence the travel of radio waves (Wahi et al., 2005; Bhattacharya et al., 2009; Mayr and Mahajan, 1971; Mahajan and Pandey, 1980). It plays a crucial role in various atmospheric and space-based communication, navigation, and remote sensing systems (Meena et al., 2024; Rishbeth and Garriott, 1969; Schunk and Nagy, 2009). It is the most important part of the Earth's atmosphere because it is the region where the Sun first interacts with. It is highly dynamical in nature due to selective absorption of solar electromagnetic radiation by the atmospheric constituents. It is a region full of active photochemical and dynamical interactions. Most of the atmospheric phenomena occur in this region. It also acts as a gateway between the Earth's environment and the space, where the Sun's energy is first deposited into the Earth's environment.

The ionosphere's structure, composition, and dynamics are heavily influenced by solar activity (Meena et al., 2024). Response of the ionosphere to the changes of solar activity is important part of the space weather issue, because of its impact on the human space-based activity (Kutiev et al., 2013). The variations in solar activity causes considerable fluctuations in the ionosphere, affecting neutral density and temperature, as well as ion and electron densities, temperatures, neutral winds, and electric fields (Momeni and Migoya-Orue, 2025; Kusano, 2023; Gorney, 1990; Liu et al., 2011; Liu and Wan, 2020). Moreover, understanding the ionosphere's dependence on solar activity is crucial for the development of accurate empirical ionospheric models (Benella et al., 2023, Migoya-Orué et al., 2017, Radicella et al., 2021). The study of ionospheric climatology, particularly the influence of solar activity, offers crucial information on ionospheric weather patterns (Wang et al., 2021, Jakowski et al., 2012). However, it is one of the least explored parts of the atmosphere owing to the difficulties in making direct observations from the ground. There are very less studies available to understand the variation

ISSN No. 2454-6194 | DOI: 10.51584/IJRIAS |Volume X Issue XII December 2025

of ionosphere in both the hemisphere during various solar activity conditions. In this paper, we have studied the response of the Earth's ionosphere to solar activity during minimum, moderate and maximum conditions during the solar cycle 24 in both the hemispheres with the help of well-developed and verified empirical model namely IRI-2016 model (Bilitza et al., 2017).

Model

Empirical models of the Earth's ionosphere are an indispensable tool used by scientific communities for data analysis, initialization of detailed physics-based models, and mission and instrument design. For over decades, the empirical models of choice among scientists have been the IRI model for ionosphere. The IRI-2016 model is freely accessible online database model and it was built as an empirical model representing the syntheses of most of the available ground and space measurements of ionospheric characteristics. This model is used in the present study to obtain the ion densities, electron density, ion and electron temperatures.

International Reference Ionosphere 2016 (IRI-2016) Model

The IRI-2016 was developed by Bilitza et. al. 2017. The IRI is an international project sponsored by the Committee on Space Research (COSPAR) and the International Union of Radio Science (URSI) with the goal of developing and improving an international standard for the parameters in Earth's ionosphere (Bilitza et al., 2014). These organizations formed a Working Group in the late sixties to produce an empirical standard model of the ionosphere, based on all available data sources. Several steadily improved editions of the model have been released (Bilitza, 2018). For given location, time and date, IRI provides monthly averages of the electron density, electron temperature, ion temperature, and ion composition in the ionospheric altitude range. In the present study, we have obtained the altitude profiles (60-500km) of ion densities, electron density, ion temperature and electron temperature from the IRI-2016 model during the solar cycle 24 for minimum (F10.7 = 69.8 on 4 January 2020), moderate (F10.7 = 131.6 on 4 January 2012) and maximum (F10.7 = 253.3 on 4 January 2014) solar activity conditions at 45º latitude and 180º longitude in both the hemispheres for 12 noon local time.

RESULTS AND DISCUSSION

The altitude profiles of ion densities (O_2^+, NO^+, N^+, O^+), electron density (N_e), ion temperature (T_i) and electron temperature (T_e) are obtained from the IRI-2016 model on 4 January 2020 (F10.7 = 69.8, minimum), 4 January 2012 (F10.7 = 131.6, moderate) and 4 January 2014 (F10.7 = 253.3, maximum) at 45º latitude and 180º longitude in both the hemispheres for 12 noon local time from 60km to 500 km altitude.

Ion Densities and Ion Temperature

Figure 1 shows the altitude profiles of O_2^+ density from 60 to 500 km obtained from IRI-2016 model on 4 January 2020 (minimum, F10.7=69.8), 4 January 2012 (moderate, F10.7=131.6 and 4 January 2014 (maximum, F10.7=253.3) in north hemisphere (top panel) and in south hemisphere (middle panel) at 45° latitude and 180° longitude at 12 noon local time. The ratio of O_2^+ density in north to south is also shown in bottom panel of Figure 1. It can be noticeable from Figure 1 (top and middle panels) that the altitude profile of O_2^+ density shows two peaks, one at 100km and another at about 175km. The O_2^+ density is more or less same at all altitudes in north hemisphere (top panel) during minimum, moderate and maximum solar activity conditions. In southern hemisphere (middle panel), the O_2^+ density is more or less same between 60km to 125km, above 125km a significant variation can be noticed during minimum, moderate and maximum solar activity conditions. The O_2^+ density is deceased as solar activity increased from minimum to maximum between 125 km and 200km (middle panel). Further, the O_2^+ density increased as solar activity increased from minimum to maximum above 200km. Figure 1(bottom panel) shows the relative variation of O_2^+ density in northern hemisphere in compare with southern hemisphere. It can be noticed from Figure 1 (bottom panel) that the O_2^+ density is more in southern hemisphere in compare with northern hemisphere at all altitudes below 100km and above 200km. Between 100km and 200km, the O_2^+ density is more in northern hemisphere in compare with southern hemisphere.

ISSN No. 2454-6194 | DOI: 10.51584/IJRIAS |Volume X Issue XII December 2025

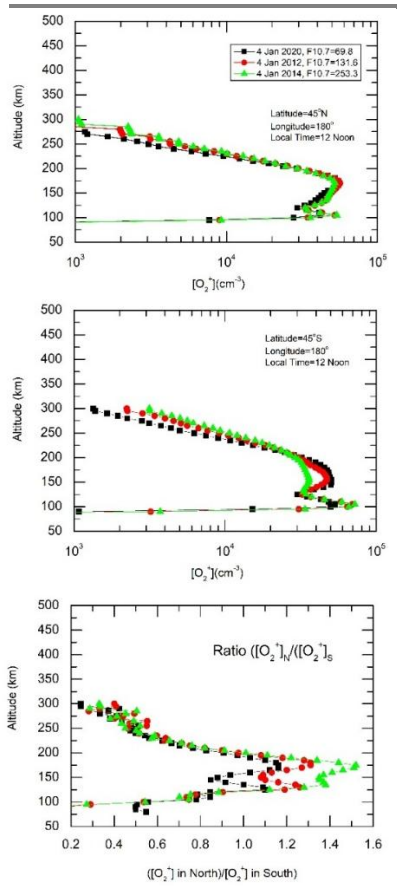

Figure 1: Altitude profiles of O_2^+ density obtained from IRI-2016 model on 4 January 2020 (minimum, F10.7=69.8), 4 January 2012 (moderate, F10.7=131.6) and 4 January 2014 (maximum, F10.7=253.3) in north hemisphere (top panel) and in south hemisphere (middle panel) at 45° latitude and 180° longitude at 12 noon local time. (Bottom panel) the relative variation of O_2^+ density in north hemisphere in compare with south hemisphere.

Figure 2 shows the altitude profiles of NO^+ density from 60 to 500 km obtained from IRI-2016 model on 4 January 2020 (minimum, F10.7=69.8), 4 January 2012 (moderate, F10.7=131.6 and 4 January 2014 (maximum, F10.7=253.3) in north hemisphere (top panel) and in south hemisphere (middle panel) at 45° latitude and 180° longitude at 12 noon local time. The ratio of NO^+ density in north to south is also shown in bottom panel of Figure 2. It can be noticeable from Figure 2 (top and middle panels) that the NO^+ density is more or less same between 60km and 100km in both hemispheres (top and middle panels). It can also noticeable from Figure 2 (top and middle panels) that the NO^+ density shows a significant variation at above 100km. The direct correlation can be noticed between the NO^+ density and the solar activity above 100km that the NO^+ density increased as the solar activity increased from minimum to maximum solar activity. Figure 2(bottom panel) shows the relative variation of NO^+ density in northern hemisphere in compare with southern hemisphere. It can be noticed from Figure 2 (bottom panel) that the NO^+ density is more in southern hemisphere in compare with northern hemisphere at all altitudes.

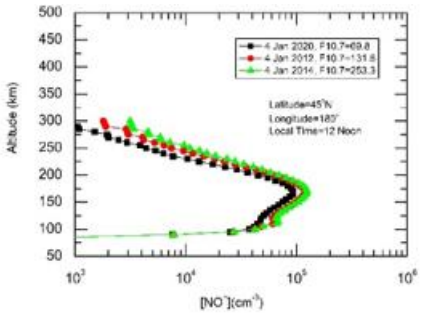

ISSN No. 2454-6194 | DOI: 10.51584/IJRIAS |Volume X Issue XII December 2025

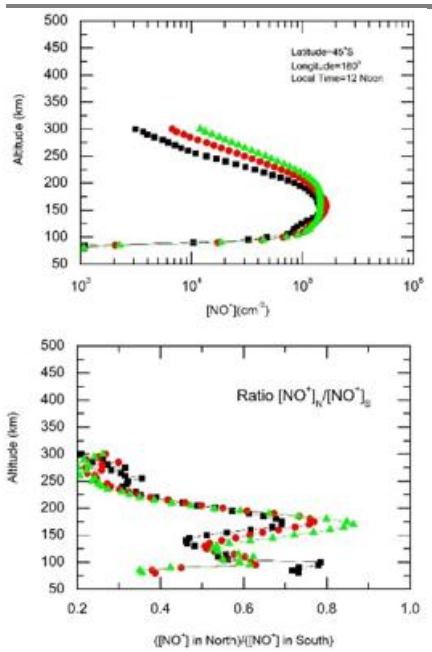

Figure 2: Altitude profiles of NO^+ density obtained from IRI-2016 model on 4 January 2020 (minimum, F10.7=69.8), 4 January 2012 (moderate, F10.7=131.6) and 4 January 2014 (maximum, F10.7=253.3) in north hemisphere (top panel) and in south hemisphere (middle panel) at 45° latitude and 180° longitude at 12 noon local time. (Bottom panel) the relative variation of NO^+ density in north hemisphere in compare with south hemisphere.

Figure 3 shows the altitude profiles of N^+ density obtained from IRI-2016 model on 4 January 2020 (minimum, F10.7=69.8), 4 January 2012 (moderate, F10.7=131.6 and 4 January 2014 (maximum, F10.7=253.3) in north hemisphere (top panel) and in south hemisphere (middle panel) at 45° latitude and 180° longitude at 12 noon local time. The ratio of N^+ density in north to south is also shown in bottom panel of Figure 3. It can be noticeable from Figure 3 (top and middle panels) that the N^+ density varies significantly during minimum, moderate and maximum solar activity conditions. The N^+ density increased with solar activity. It can be noticed from Figure 3 relative variation (bottom panel) that the N^+ density is more in southern hemisphere in compare with northern hemisphere below 300km and above 400km. The N^+ density is more in northern hemisphere in compare with the southern hemisphere between 300km and 400km.

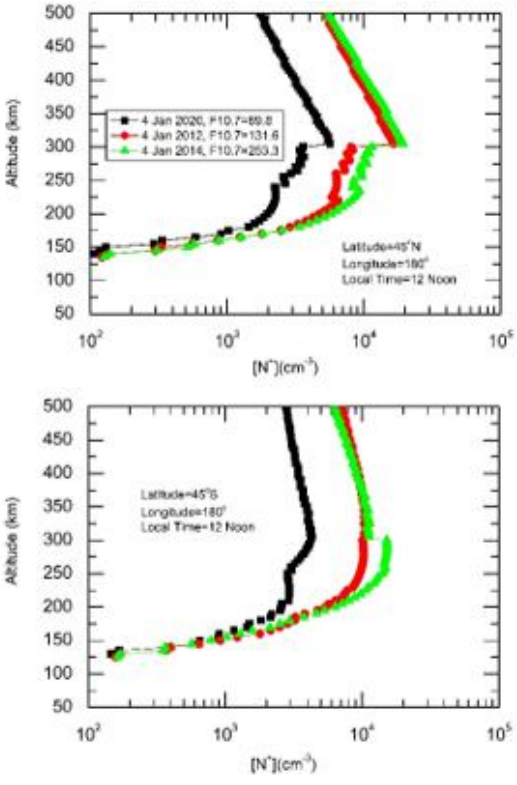

ISSN No. 2454-6194 | DOI: 10.51584/IJRIAS |Volume X Issue XII December 2025

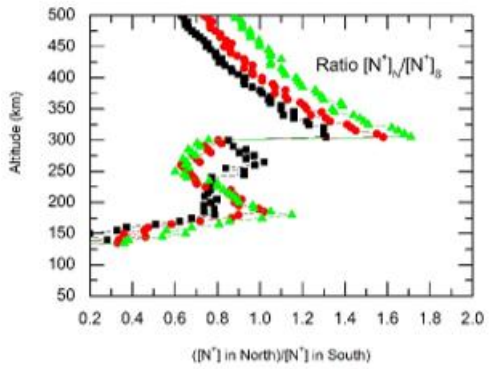

Figure 3: Altitude profiles of N^+ density obtained from IRI-2016 model on 4 January 2020 (minimum, F10.7=69.8), 4 January 2012 (moderate, F10.7=131.6) and 4 January 2014 (maximum, F10.7=253.3) in north hemisphere (top panel) and in south hemisphere (middle panel) at 45° latitude and 180° longitude at 12 noon local time. (Bottom panel) the relative variation of N^+ density in north hemisphere in compare with south hemisphere.

The altitude profiles of O^+ density obtained from IRI-2016 model on 4 January 2020 (minimum, F10.7=69.8), 4 January 2012 (moderate, F10.7=131.6 and 4 January 2014 (maximum, F10.7=253.3) in north hemisphere (top panel) and in south hemisphere (middle panel) at 45° latitude and 180° longitude at 12 noon local time are shown in Figure 4. The ratio of O^+ density in north to south is also shown in bottom panel of Figure 4. It can be noticeable from Figure 4 (top and middle panels) that the O^+ density shows a significant variation during minimum, moderate and maximum solar activity conditions. The O^+ density increased with solar activity. It can be noticed from Figure 4 relative variation (bottom panel) that the O^+ density is more in northern hemisphere in compare with southern hemisphere above 150km. Below 150km, the O^+ density is more in southern hemisphere in compare with the northern hemisphere.

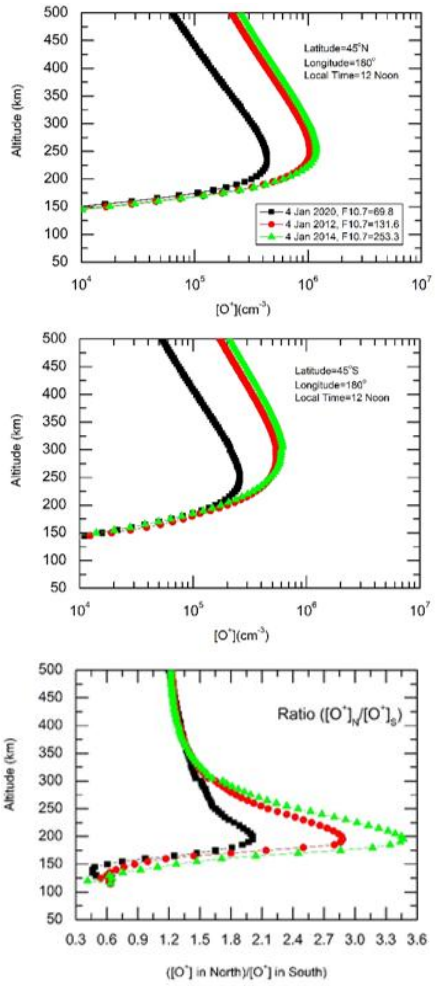

Figure 4: Altitude profiles of O^+ density obtained from IRI-2016 model on 4 January 2020 (minimum,

ISSN No. 2454-6194 | DOI: 10.51584/IJRIAS |Volume X Issue XII December 2025

F10.7=69.8), 4 January 2012 (moderate, F10.7=131.6) and 4 January 2014 (maximum, F10.7=253.3) in north hemisphere (top panel) and in south hemisphere (middle panel) at 45° latitude and 180° longitude at 12 noon local time. (Bottom panel) the relative variation of O^+ density in north hemisphere in compare with south hemisphere.

Figure 5 shows the altitude profiles of ion temperature (T_i) obtained from IRI-2016 model on 4 January 2020 (minimum, F10.7=69.8), 4 January 2012 (moderate, F10.7=131.6 and 4 January 2014 (maximum, F10.7=253.3) in north hemisphere (top panel) and in south hemisphere (middle panel) at 45° latitude and 180° longitude at 12 noon local time. The ratio of T_i in north to south is also shown in bottom panel of Figure 5. It can be noticeable from Figure 5 (top and middle panels) that the T_i shows a significant variation between 150km and 450km during minimum, moderate and maximum solar activity conditions. The direct correlation is found between T_i and solar activity between 150km and 450km. Below 150km and above 450km, the T_i is more or less same during three solar activity conditions. It can be noticed from Figure 5 relative variation (bottom panel) that the T_i is more in southern hemisphere in compare with northern hemisphere at almost all altitudes.

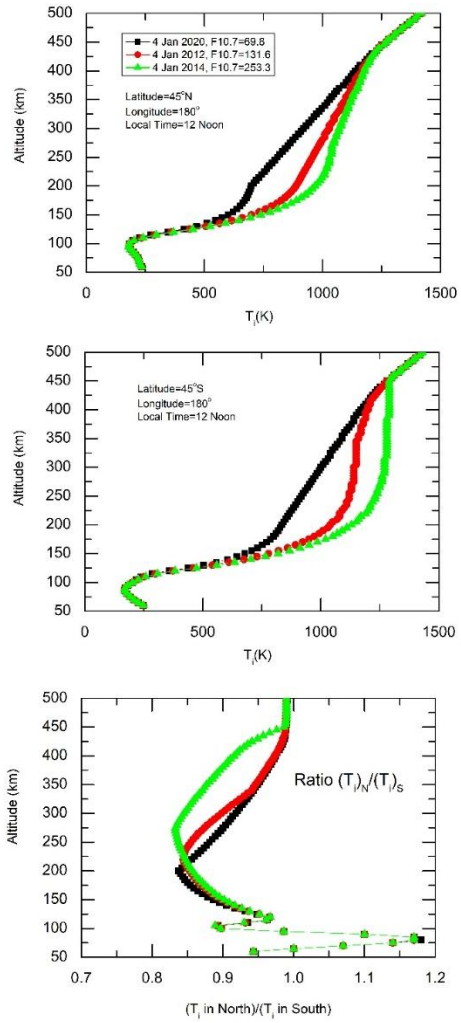

Figure 5: Altitude profiles of ion temperature (T_i) obtained from IRI-2016 model on 4 January 2020 (minimum, F10.7=69.8), 4 January 2012 (moderate, F10.7=131.6) and 4 January 2014 (maximum, F10.7=253.3) in north hemisphere (top panel) and in south hemisphere (middle panel) at 45° latitude and 180° longitude at 12 noon local time. (Bottom panel) the relative variation of ion temperature (T_i) in north hemisphere in compare with south hemisphere.

Electron density and electron temperature

Figure 6 shows the altitude profiles of electron density (N_e) obtained from IRI-2016 model on 4 January 2020 (minimum, F10.7=69.8), 4 January 2012 (moderate, F10.7=131.6 and 4 January 2014 (maximum, F10.7=253.3) in north hemisphere (top panel) and in south hemisphere (middle panel) at 45° latitude and 180° longitude at 12 noon local time. The ratio of N_e in north to south is also shown in bottom panel of Figure 6. It can be noticeable from Figure 6 (top and middle panels) that the electron profile shows two peaks, one at 100km and other at about

ISSN No. 2454-6194 | DOI: 10.51584/IJRIAS |Volume X Issue XII December 2025

250km. The N_e shows a significant variation during minimum, moderate and maximum solar activity conditions. The direct correlation can be seen between N_e and solar activity. It can be noticed from Figure 6 relative variation (bottom panel) that the N_e is more in northern hemisphere in compare with southern hemisphere above 150km. Below 150km, the N_e is more in southern hemisphere in compare with the northern hemisphere.

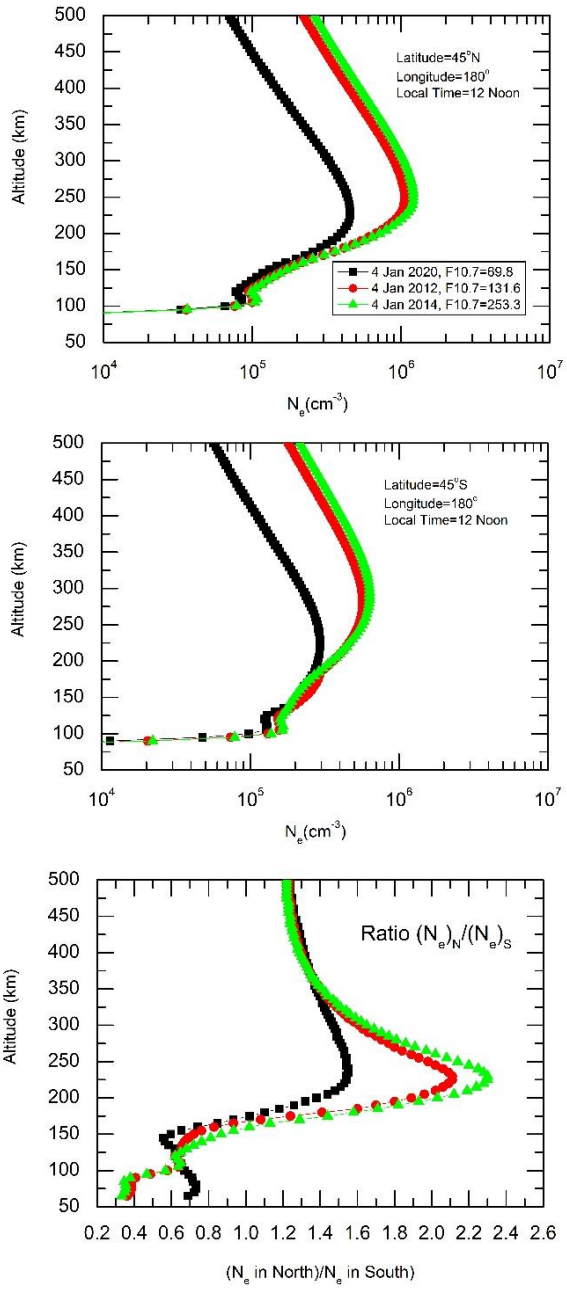

Figure 6: Altitude profiles of electron density (N_e) obtained from IRI-2016 model on 4 January 2020 (minimum, F10.7=69.8), 4 January 2012 (moderate, F10.7=131.6) and 4 January 2014 (maximum, F10.7=253.3) in north hemisphere (top panel) and in south hemisphere (middle panel) at 45° latitude and 180° longitude at 12 noon local time. (Bottom panel) the relative variation of electron density (N_e) in north hemisphere in compare with south hemisphere.

Figure 7 shows the altitude profiles of electron temperature (T_e) obtained from IRI-2016 model on 4 January 2020 (minimum, F10.7=69.8), 4 January 2012 (moderate, F10.7=131.6 and 4 January 2014 (maximum, F10.7=253.3) in north hemisphere (top panel) and in south hemisphere (middle panel) at 45° latitude and 180° longitude at 12 noon local time. The ratio of T_e in north to south is also shown in bottom panel of Figure 7. It can be noticeable from Figure 7 (top and middle panels) that the T_e is more or less same below 250km in northern hemisphere and below 350km in southern hemisphere. The T_e shows a significant variation above 250km in north latitude and above 350km in south latitude during minimum, moderate and maximum solar activity conditions. It can be noticed from Figure 7 relative variation (bottom panel) that the T_e is more in southern hemisphere in compare with northern hemisphere at almost all altitudes.

ISSN No. 2454-6194 | DOI: 10.51584/IJRIAS |Volume X Issue XII December 2025

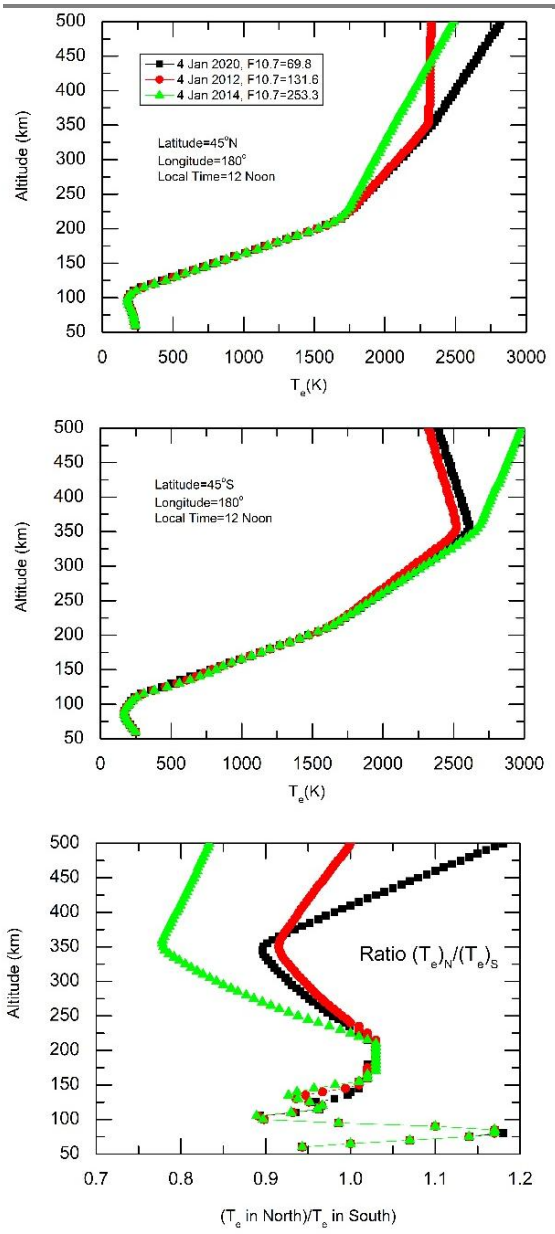

Figure 7: Altitude profiles of electron temperature (T_e) obtained from IRI-2016 model on 4 January 2020 (minimum, F10.7=69.8), 4 January 2012 (moderate, F10.7=131.6) and 4 January 2014 (maximum, F10.7=253.3) in north hemisphere (top panel) and in south hemisphere (middle panel) at 45° latitude and 180° longitude at 12 noon local time. (Bottom panel) the relative variation of electron temperature (T_e) in north hemisphere in compare with south hemisphere.

CONCLUSION

The response of the Earth's ionosphere to solar radiation is studied during minimum, moderate, and maximum solar activity conditions at 45° latitude and 180° longitude at 12 noon local time in both hemispheres with the help of IRI-2016 model. It is found that ion densities, ion temperature, electron density and electron temperature show a significate variation under varying solar activity conditions. The direct correlation is found between ionospheric parameters and solar activity at most of the altitudes. It is also found that the O^+ and electron density are more in northern hemisphere than in southern hemisphere. Further, the results show that the ion densities (O_2^+, NO^+, N^+), ion and electron temperatures (T_e, T_i) are more in southern hemisphere in compare with the northern hemisphere.

ACKNOWLEDGEMENT

Authors acknowledge the IRI working group for making data freely available for scientific purpose. The data used in this study is obtained from the IRI-2016 model and can be found at http://irimodel.org/.

REFERENCES

1. Benella, S., Quattrociocchi, V., Papini, E., et al. (2023). Modeling turbulent fluctuations in high-latitude ionospheric plasma using electric field cses-01 observations. Atmosphere 14(9), 1466. https://doi.org/10.3390/atmos14091466.
2. Bhattacharya, S., Purohit, P.K., and Gwal, A.K. (2009). Ionospheric time delay variations in the equatorial anomaly region during low solar activity using GPS. Ind. J. Radio. Space. Phys., 38, 266-274.
3. Bilitza, D. (2018). IRI the International Standard for the Ionosphere, Adv. Radio Sci., 16, 1–11. https://doi.org/10.5194/ars-16-1-2018.
4. Bilitza, D., Altadill, D., Truhlik, V., Shubin, V., Galkin, I., Reinisch, B., and Huang, X. (2017). International Reference Ionosphere 2016: From ionospheric climate to real-time weather predictions, Space Weather, 15, 418–429. doi:10.1002/2016SW001593.
5. Bilitza, D., Altadill, D., Zhang, Y., Mertens, C., Truhlik, V., Richards, P., McKinnell, L.-A., and Reinisch, B. (2014). The International Reference Ionosphere 2012 – a model of international collaboration, J. Space Weather Space Climate, 4, 1–12. https://doi.org/10.1051/swsc/2014004.
6. Gorney, D. (1990). Solar cycle effects on the near-earth space environment. Rev. Geophys. 28(3), 315-336. https://doi.org/10.1029/ RG028i003p00315.
7. Jakowski, N., Be´niguel, Y., De Franceschi, G., et al. (2012). Monitoring, tracking and forecasting ionospheric perturbations using gnss techniques. J. Space Weather Space Clim. 2, A22. https://doi.org/10.1051/swsc/2012022.
8. Kusano, K. (2023). Solar-terrestrial environmental prediction. Springer.
9. Kutiev, I., Tsagouri, I., Perrone, L., Pancheva, D., Mukhtarov, P., Mikhailov, A., Lastovicka, J., Jakowski, N., Buresova, D., Blanch, E., Andonov, B., Altadill, D., Magdaleno, S., Parisi, M., and Miquel Torta, J. (2013). Solar activity impact on the Earth's upper atmosphere. J. Space Weather Space Clim., 3, A06.
10. Liu, L., and Wan, W. (2020). Recent ionospheric investigations in china (2018–2019). Earth Planet. Phys. 4 (3), 179–205. https://doi.org/10.26464/epp2020028.
11. Liu, L., Wan, W., Chen, Y., et al. (2011). Solar activity effects of the ionosphere: A brief review. Chin. Sci. Bull. 56, 1202–1211. https://doi. org/10.1007/s11434-010-4226-9.
12. Mahajan, K. K., and V.K. Pandey, V. K. (1980). Models of electron temperature in the topside ionosphere for low and medium solar activity conditions. J. Geophys. Res., 85, 213-216.
13. Mahdi Momeni, and Yenca Migoya-Orué (2025). Solar activity and ionospheric variation: A comprehensive study using hurst exponent and probability density functions analysis, Advances in Space Research, 75(10), 7668-7683.
14. Mayr, H. G., and Mahajan, K. K. (1971). Seasonal variation in the F2 region. J. Geophys. Res., 76, 1017-1027.
15. Meena, A. K., Sharma, A., and Gour, P. S. (2024). The impact of moderate solar flare activity on ionospheric response from august 5th to 7th, 2023. World Journal of Advanced Research and Reviews, 22(01), 043–054.
16. Migoya-Orue´, Y., Folarin-Olufunmilayo, O., Radicella, S., et al. (2017). Evaluation of nequick as a model to characterize the equatorial ionization anomaly over Africa using data ingestion. Adv. Space Res. 60(8), 1732–1738. https://doi.org/10.1016/j.asr.2017.01.013.
17. Radicella, S., Alazo-Cuartas, K., Migoya-Orue´, Y., et al. (2021). Thickness parameters in the empirical modelling of bottom side electron density profiles. Adv. Space Res. 68(5), 2069–2075. https://doi.org/10.1016/j.asr.2020.12.037.
18. Rishbeth, H., and Garriott, O. K. (1969). Introduction to ionospheric physics. International Geophysics Series, 14.
19. Schunk, R. W., and Nagy, A. F. (2009). Ionospheres: Physics, plasma physics, and chemistry. Cambridge University Press.
20. Wahi, R., Dubey, S., and Gwal, A.K. (2005). Ionospheric total electron content measurement in Malaysian region during high solar activity using GPS receiver. Ind. J. Radio. Space. Phys., 34, 399-401.
21. Wang, C., Li, Y., Wu, J., et al. (2021). An ionospheric climate index based on gnss. Space Weather 19(1). https://doi.org/10.1029/ 2020SW002596, e2020SW002 596.